

## ARTICLE INFO

## Article history:

Received 29 January 2014  
 Received in revised form 21 May 2014  
 Accepted 3 July 2014  
 Available online 9 July 2014

## Keywords:

Micro-erosion meter  
 Condensation  
 Dissolutional forms  
 Microclimate monitoring  
 Gypsum speleothems  
 Gypsum karst

## The role of condensation in the evolution of dissolutional forms in gypsum caves: Study case in the karst of Sorbas (SE Spain)

Fernando Gázquez <sup>a,\*</sup>, José-María Calaforra <sup>b</sup>, Paolo Forti <sup>c</sup>, Jo DeWaele <sup>c</sup>, Laura Sanna <sup>d</sup>

<sup>a</sup> Department of Earth Sciences, Cambridge University, Downing Street, Cambridge, Cambridgeshire CB2 3EQ, United Kingdom

<sup>b</sup> Water Resources and Environmental Geology Research Group, Dept. of Hydrogeology and Analytical Chemistry, University of Almería, Crta. Sacramento s/n, La Cañada de San Urbano, 04120 Almería, Spain

<sup>c</sup> Italian Institute of Speleology, Department of Biological, Geological and Environmental Sciences, University of Bologna, Via Zamboni, 67, 40126 Bologna, Italy

<sup>d</sup> Institute of Biometeorology, National Research Council of Italy, Traversa la Crucca 3, Regione Balduca, Li Punti, 07100 Sassari, Italy

\* Corresponding author.

E-mail addresses: [fg331@cam.ac.uk](mailto:fg331@cam.ac.uk) (F. Gázquez), [jmcalaforra@ual.es](mailto:jmcalaforra@ual.es) (J.-M. Calaforra), [paolo.forti@unibo.it](mailto:paolo.forti@unibo.it) (P. Forti), [jo.dewaele@unibo.it](mailto:jo.dewaele@unibo.it) (J. DeWaele), [speleokikers@tiscali.it](mailto:speleokikers@tiscali.it) (L. Sanna).

<http://dx.doi.org/10.1016/j.geomorph.2014.07.006>

### ABSTRACT

The karst of Sorbas (SE Spain) is one of the most important gypsum areas worldwide. Its underground karst network comprises over 100 km of cave passages. Rounded smooth forms, condensation cupola and pendant-like features appear on the ceiling of the shallower passages as a result of gypsum dissolution by condensation water. Meanwhile, gypsum speleothems formed by capillarity, evaporation and aerosol deposition such as coralloids, gypsum crusts and rims are frequently observed closer to the passage floors. The role of condensation–dissolution mechanisms in the evolution of geomorphological features observed in the upper cave levels has been studied by means of long-term micro-erosion meter (MEM) measurements, direct collection and analysis of condensation waters, and micrometeorological monitoring. Monitoring of erosion at different heights on gypsum walls of the Cueva del Agua reveals that the gypsum surface retreated up to 0.033 mm yr<sup>-1</sup> in MEM stations located in the higher parts of the cave walls. The surface retreat was negligible at the lowest sites, suggesting higher dissolution rates close to the cave ceiling, where warmer and moister air flows. Monitoring of microclimatic parameters and direct measurements of condensation water were performed in the Covadura Cave system in order to estimate seasonal patterns of condensation. Direct measurements of condensation water dripping from a metal plate placed in the central part of the El Bosque Gallery of Covadura Cave indicate that condensation takes place mainly between July and November in coincidence with rainless periods. The estimated gypsum surface lowering due to this condensation water is 0.0026mmyr<sup>-1</sup>. Microclimatic monitoring in the same area shows differences in air temperature and humidity of the lower parts of the galleries (colder and drier) with respect to the cave ceiling (warmer and wetter). This thermal sedimentation controls the intensity of the condensation–evaporation mechanisms at different heights in the cave.

### 1. Introduction

Subterranean morphologies in caves have been utilised in many cases to identify the type of speleogenetic mechanisms involved in the endokarst development, especially to distinguish between epigenic and hypogenic speleogenesis (Klimchouk, 2009; Palmer, 2011). Subaqueous speleogenesis produces typical cave morphologies, including scallops, cupolas (rounded ceiling pockets), ceiling channels, pendants, oxidation vents, bubble trails and zenithal ceiling tubes, described in a variety of caves (Audra et al., 2002; Calaforra and Pulido-Bosch, 2003; De Waele and Forti, 2006; Audra et al., 2007, 2009; Klimchouk, 2009; Calaforra and De Waele, 2011; Palmer, 2011; Pasini, 2012; Gázquez and Calaforra, 2013, amongst others).

Subaerial speleogenesis may occur in caves placed above the water table. Condensation and CO<sub>2</sub> diffusion into the condensed water, termed “condensation corrosion” by Ford and Williams (1989), is identified as being the precursor process of carbonate rock dissolution both in nonthermal (Jameson, 1991; Tarhule-Lips and Ford, 1998; De Freitas and Schmekal, 2006) and thermal caves, which display specific dissolution patterns (Cigna and Forti, 1986; Bakalowicz et al., 1987; Sarbu and Lascu, 1997; Audra et al., 2007; Gázquez et al., 2013). Some characteristic speleogen features produced by condensation corrosion are “air scallops” (Hill, 1987), hollow half-spheres on walls and ceilings (Cigna and Forti, 1986; DeWaele et al., 2009; Plan et al., 2012), boxwork formations (LaRock and Cunningham, 1995; Gázquez et al., 2012), weathering rinds (Auler and Smart, 2004), and less frequently, corrosion channels (Vattano et al., 2013).

Condensation corrosion can pose a serious threat for the conservation of the subterranean heritage, in particular in show caves in which microclimatic conditions are artificially altered by visitors. Modification of cave air temperature, humidity and particularly CO<sub>2</sub> concentration in air can trigger dissolution–corrosion of speleothems (Dublyansky and Dublyansky, 2000; Avramidis et al., 2001; Fernández-Cortés et al., 2006).

Condensation is a widespread process in caves, as revealed by the large number of research works published over the past thirty years, based on direct or indirect measurements of this phenomenon (Cigna and Forti, 1986; Sarbu and Lascu, 1997; Dublyansky and Dublyansky, 1998; Tarhule-Lips and Ford, 1998; Avramidis et al., 2001; De Freitas and Schmekal, 2003; Auler and Smart, 2004; De Freitas and Schmekal, 2006). Suspended glass plates (Sarbu and Lascu, 1997), lysimeters and metallic devices (Dublyansky and Dublyansky, 1998), refrigerated containers (Tarhule-Lips and Ford, 1998), weight loss measurements of gypsum tablets (Calaforra, 1996; Klimchouk et al., 1996; Klimchouk and Aksem, 2002; Tarhule-Lips and Ford, 1998), micro-erosion meter measurements of cave surface retreatment (Calaforra et al., 1993; Klimchouk et al., 1996), determining thickness and age of weathering rinds (Auler and Smart, 2004), and more recently electrical devices coupled to data loggers (De Freitas and Schmekal, 2006) have been

utilised to estimate and/or measure condensation in caves. In addition, theoretical models and approaches to the condensation mechanisms in caves have been developed over the last decade (Dreybrodt et al., 2005; Gabrovšek et al., 2010).

Condensation corrosion has been postulated as an important process in speleogenesis in semi-desertic karst areas of Central Asia (Dublyansky and Dublyansky, 1998), northeastern Brazil (Auler and Smart, 2004) and the Mediterranean region (Pasquini, 1973; De Waele et al., 2009). Dublyanskaya and Dublyansky (1989) argued that at a global scale, the possibility of condensation in caves strongly depends on latitude and altitude.

Remarkably, condensation studies in non-carbonate caves have been very limited and scarce (Calaforra et al., 1993; Klimchouk et al., 1996; Fernández-Cortés et al., 2006), mainly focused on gypsum environments.

Because of the fact that the ratio of gypsum to calcite solubility is around 10:1 (Ford and Williams, 1989), the effects of condensation corrosion in gypsum caves are presumably greater than those experienced in carbonate caves. Therefore, cave morphologies produced by condensation are of major relevance for vadose speleogenesis in gypsum caves with respect to limestone caves (Calaforra et al., 1993). Moreover, the aggressiveness of the condensed water in gypsum caves is not affected by the CO<sub>2</sub> diffusion from air to water that is the slowest reaction in the dissolution kinetics of condensation corrosion in carbonate systems.

Another relevant line of research deals with the importance of condensation in the total recharge of gypsum aquifers, in particular in semi-arid areas. Various research works have postulated that condensation can represent a substantial contribution to the total recharge in gypsum aquifers (Calaforra et al., 1993; Forti, 1993) and can play an important role in the dry-season discharge of karst springs and rivers (Dublyansky and Dublyansky, 1998).

In the present work, various morphological features induced by condensation–dissolution mechanisms have been studied in several shallow caves of the gypsum karst of Sorbas (Almería, SE Spain), one of the most well-known gypsum karst areas of the world (Calaforra and Pulido-Bosch, 1996, 2003; Gázquez and Calaforra, 2014). In the Cueva del Agua, the longest gypsum cave in Spain, micro-erosion meter (MEM) measurements of gypsum wall retreat over the past twenty years have suggested condensation corrosion to be effective, besides normal erosion. Monitoring microclimatic parameters (temperature and relative humidity) and direct measurements of condensation water were performed in the upper levels of Covadura Cave during the period 2011–2013, in order to identify seasonal patterns of condensation–evaporation mechanisms and their effects on the gypsum cave morphology during recent vadose stages.

## 2. Geological setting and cave description

### 2.1. Geology

The gypsum karst of Sorbas (Almería, SE Spain) is one of the best known karst areas in Spain (Calaforra and Pulido-Bosch, 2003). Nearly one thousand caves are concentrated in only 25 km<sup>2</sup>, forming one of the most important gypsum karst areas in the world from the cave science perspective.

The gypsum karst of Sorbas is located in the Tabernas–Sorbas Basin, SE Spain, one of the intramontane Neogene basins within the Betic Cordillera. It includes significant gypsiferous Messinian evaporites in its sedimentary fill (Dronkert, 1977). It lies within a topographic depression bounded to the north by the Filabres Range and to the south by the Alhamilla and Cabrera ranges (Fig. 1). The region has a semiarid climate, with mean annual precipitation around 300 mm (Maestre et al., 2013).

The karstified Messinian gypsum (Yesares Member) occurs as a 120 m thick cyclic sequence consisting of alternating gypsum and pelitic–marly units (Dronkert, 1977). The selenitic gypsum units reach 30 m in thickness. The most complete sequence of the Yesares Member crops out in the Río Aguas canyon, where 12 cycles of alternating gypsiferous and carbonate–pelitic laminated sediments were initially described by Dronkert (1976), though up to 14 (Krijgsman et al., 2001) and 16 (Roveri et al., 2009) sedimentary cycles were recognised in later works. Such stratigraphic alternation has been attributed to precessional cycles of the Earth with impact on the global climate (Krijgsman et al., 2001). The Messinian sequence is scarcely deformed in the centre of the basin, barely affected by minor tilting and faulting. Stratification of the gypsum–marl series and diaclasses played a decisive role in the development and configuration of the cave levels (Calaforra and Pulido-Bosch, 2003).

The Yesares Member is overlain by (1) marine sandstones with some intercalated siltstones of the Sorbas Member (Roep et al., 1979); (2) coastal plain silts and sands of the Zorreras Member; and (3) continental conglomerates of the Góchar Formation (Mather et al., 2001). The semi-pervious nature of the overlying sequence was of great importance for the development of the gypsum karst, as it creates semiconfined conditions on the gypsum strata at the western edge of the basin and controls the hydrogeological regime of the main spring of Los Molinos (Calaforra, 1996). The impervious base of the gypsum aquifer comprises silts and clays of the Abad Member.

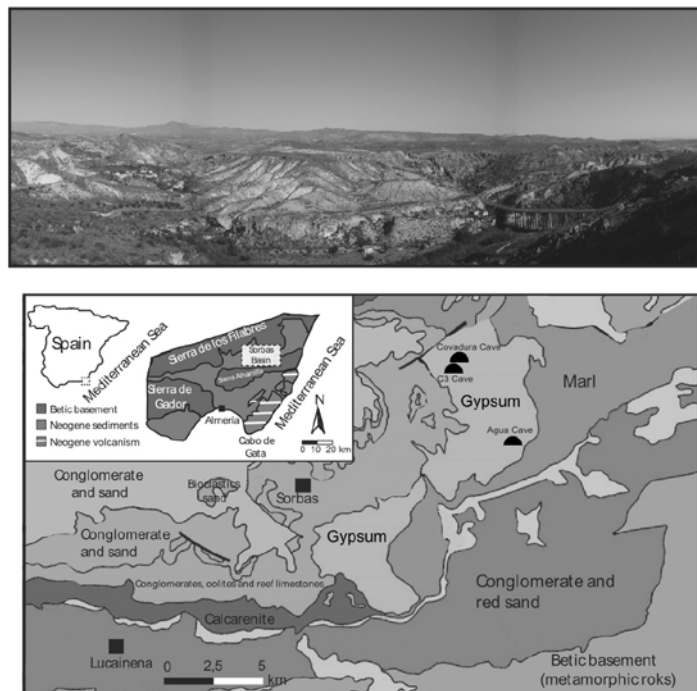


Fig. 1. Panoramic view of the gypsum karst of Sorbas (above) and geological sketch of the Sorbas Basin (below) (modified from Braga et al., 2003). Location of the studied cave (photo by L. Sanna).

## 2.2. Caves

Up to six passage levels have been detected in the gypsum caves. Their development was controlled by the stratification planes between the soft marls and the more soluble gypsum units. This cave arrangement is related to the hydrogeological history of the area. Initially, the gypsum karst evolved as a semi-confined multi-layer aquifer under phreatic conditions, enabling the formation of small proto-conduits in individual gypsum beds, whilst the marly and clayey interbeds acted as impervious barriers (Calaforra and Pulido-Bosch, 2003).

During a subsequent stage, after lowering of the piezometric level following fluvial incision, vadose conditions were established and mechanical erosion in the underlying marls and clays became the dominant process. This genetic duality indicates that the Sorbas gypsum karst can be considered an example of interstratal karstification, in which underground erosion processes and the resulting features should be considered products of the hydrogeological evolution (Calaforra and Pulido-Bosch, 2003).

Most cave passages of the gypsum karst of Sorbas show a predominantly horizontal attitude, and have relatively low vertical development (less than 10 m in many cases), as well as multiple entrances (Calaforra and Pulido-Bosch, 2003). This is the case of Covadura Cave, on the north-western part of the gypsum karst (Fig. 2A). This cave system comprises 4.25 km of galleries distributed in six levels of depth, reaching -126 m deep. It has seven main entrances, though earlier microclimatic studies suggest possible existence of hidden air entrances, with strong influence on the air movements in the cave (Fernández-Cortés, 2005). In the upper cave levels (mainly the first and second levels of depth, less than 20 m deep) relatively intense airflow within the galleries favours evaporation, producing subaerial gypsum precipitation in the form of speleothems (Calaforra et al., 2008; Gázquez et al., 2011; Gázquez, 2012). Particularly striking are the hollow stalagmites of the El Bosque Gallery (Forest Gallery) (Fig. 3D) (Calaforra and Forti, 1993; Calaforra, 1996; Forti, 1996; Calaforra, 2003; Gázquez and Calaforra, 2014). This passage, 100 m long, is developed in the second marly stratum of the Yesares Member (around 15 m below the surface). The maximum gallery height, around 2.5 m, occurs at 20 m from the entrances, and the passage progressively decreases its size until access is not possible anymore (Fig. 2A).

The Cueva C3 is located in the northern part of the gypsum karst (Fig. 1). Its entrance lies 200 m away from the western access to Covadura Cave and 500 m from El Bosque Gallery. Despite their relatively short distance apart, a person-sized connection between these cavities has still not been found. This cave is developed in the upper marls level of the Yesares formation - around 3 m deep - and is 150 m long (Fig. 2C). The height of its passages ranges between 1.5 and 3 m. The presence of laminated detrital sediments suggests that this cave was affected by flood events in the past (Sanna et al., 2011). A variety of gypsum speleothems has been described in this cavity, including deflected stalactites, "gypsum trees", coralloids, rims and gypsum rusts (Fig. 3C, E, F, G) (Calaforra, 2003; Gázquez et al., 2011; Gázquez, 2012; Gázquez and Calaforra, 2014).

The Cueva del Agua lies on the north-eastern side of the Sorbas plateau. This cave comprises up to 8.9 km of galleries and is the longest gypsum cave in Spain. In the surroundings of the Cueva del Agua more than one hundred dolines have been mapped in an area covering 1 km<sup>2</sup>, which represents the highest density of dolines reported in Spain (Calaforra and Pulido-Bosch, 1996). The cave - comprising labyrinthine passages - has more than 33 entrances, reaching 50 m deep (Fig. 2B). A subterranean river runs through Cueva del Agua, so that some cave passages are permanently flooded. Nevertheless, there are many abandoned passages in which no evidence of recent water flows has been observed. Water springs up through the only horizontal cave entrance, located on the eastern side of the gypsum massif, giving rise to the Las Viñicas outlet that is the main entrance of this cave system. This spring drains a wide endorheic basin 1.5 km<sup>2</sup> in size and its discharge varies from less than 1 to 150 L/s, displaying fast responses to rainstorms in this area (Calaforra et al., 1993).

Air circulation inside this cave is complex and driven by thermal disequilibrium between outside air and in-cave air and water temperatures. The annual mean temperature in the main gallery oscillates around 15–7 °C, whereas the average water temperature is 14.5 °C (Calaforra et al., 1993). The cave morphology is also characterised by condensation corrosion features such as bell-shaped domes and boxwork in the cave roof. In the non-flooded galleries it is possible to find a variety of gypsum speleothems, whilst carbonate flowstones are frequently found in the hydrodynamically active sector (Calaforra, 2003; Calaforra et al., 2008).

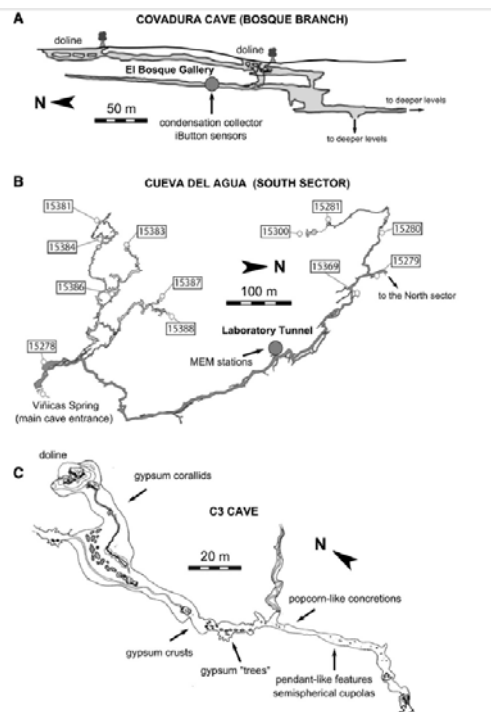


Fig. 2. Topography of the studied cave, location of the experimental stations and main speleogen features; A. profile view of El Bosque Gallery (Covadura Cave); B. plan view of Cueva del Agua (south sector), where labelled red circles represent natural entrances; C. plan view of C3 Cave, showing the most relevant speleogen features related to condensation and evaporation mechanisms. Espeleoclub Almería is credited for the topographies.

## 3. Methodology

### 3.1. Micro-erosion meter (MEM)

The micro-erosion meter (MEM) method consists in a millesimal resolution micrometer gauge (with graduations of 0.005 mm) on a tripod structure. The instrument couples to three stainless steel nails that were previously drilled into the rock surface. Two of the nails display semi-spherical head, whilst the head of the third one is flat. The micrometer gauge has three legs that perfectly fit on the three nails on the wall. Consequently, measurements are performed every time on the central part of the triangle formed by these fixed reference points.

Direct measurements of gypsum surface retreat using a MEM instrument were carried out in Cueva del Agua over a very long period. The MEM measurements inside the cave started in June 1992 and were performed five times during the 21.4 years of monitoring: the first one after a short period in October 1992, the second one in January 1994, the third one over thirteen years later (April 2007), a fourth in July 2010 (18 years) and the last one in November 2013 (Table 1).

To verify that condensation is an effective mechanism for gypsum surface retreat, two monitoring sites were put in place in the cave (Zone A and Zone B), consisting of three MEM stations each. The measuring points were placed in the gallery called the "Laboratory Tunnel" (Fig. 2B), a 1.5-m high fossil passage without evidence of recent water flow, unlike the main passage, in which the underground stream flows on the gypsum bedrock. The two measuring points are separated by 5 m in the same passage, which is 200 m from the nearest cave entrance. The MEM stations were placed on subvertical gypsum walls at three different heights, at 20 cm (bottom), 60 cm (middle) and 110 cm (top) from the passage floor (Fig. 4A). These MEM stations form part of a wider experimental network from which earlier results were published by Calaforra (1996) and Klimchouk et al. (1996). The first two measurements were performed with a micro-erosion meter produced at Trieste (Italy) ("Trieste 1" instrument). For the third measurement the "Bologna 1" instrument calibrated in Bologna (Italy) was used. The last two readings were carried out with a new instrument produced at the University of Almeria (Spain), but equivalent to "Bologna 1". All measurements have been standardised with respect to the last MEM instrument. Erosion measurements were taken by repeated readings, no more than two times in each site at the same time, to reduce the source of error due to the erosion performed by the probe tip on the gypsum surface and, therefore, producing an apparent lowering. However, the values reported for gypsum are more reliable than those from other kinds of less soluble rocks because their erosion rates are much greater, thus the errors are not as significant. Furthermore, uncertainties are demonstrated to be drastically reduced for long periods of observation (Spate et al., 1985). See also Stephenson and Finlayson (2009) and Stephenson et al. (2010) for more information about the MEM technique.

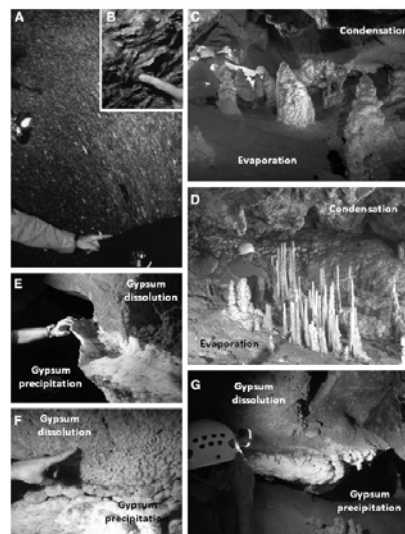


Fig. 3. Dissolutional forms and gypsum speleothems in the caves of Sorbas. A. Rounded smoothed wall in Cueva del Agua; B. gypsum crystals corroded by condensation water in Cueva del Agua; C. gypsum "trees" in C3 Cave; D. hollow stalagmites and dissolution forms on the ceiling of El Bosque Gallery of Covadura Cave; E. gypsum crusts partially dissolved in C3 Cave; F. popcorn-like speleothems showing size gradation in C3 Cave; G. pendant-like feature displaying gypsum coralloids on the lower parts (photos by Jabier Les).

Table 1  
MEM stations measurements in the "Laboratory Tunnel" of the Cueva del Agua over a period of 21.4 years.

Zone	MEM stations	20/06/1992	24/10/1992	Partial difference (0.3 yr)	20/01/1994	Partial difference (1.3 yr)	Total difference (1.6 yr)	11/04/2007	Partial difference (13.2 yr)	Total difference (14.8 yr)	27/07/2010	Partial difference (3.3 yr)	Total difference (18.1 yr)	06/11/2013	Partial difference (3.3 yr)	Total difference (21.4 yr)	Overall dissolution rate (mm yr <sup>-1</sup> )
		MEM measurement (mm)	MEM measurement (mm)		MEM measurement (mm)			MEM measurement (mm)			MEM measurement (mm)			MEM measurement (mm)			
A	Top	6.025	6.020	-0.005	6.025	0.005	0.000	5.980	-0.045	-0.045	5.880	-0.100	-0.145	5.955	-0.025	-0.070	-0.0033
A	Middle	6.685	6.675	-0.010	6.670	-0.005	-0.015	6.550	-0.120	-0.135	6.140	-0.410	-0.545	6.480	-0.070	-0.205	-0.0096
A	Bottom	9.395	9.365	-0.030	9.460	0.065	0.065	9.340	-0.120	-0.055	9.450	0.110	0.055	9.390	0.050	-0.005	-0.0002
B	Top	5.975	5.945	-0.030	5.915	-0.030	-0.060	5.810	-0.105	-0.165	5.780	-0.030	-0.195	5.270	-0.540	-0.705	-0.0330
B	Middle	7.055	7.060	0.005	6.820	-0.240	-0.235	6.690	-0.130	-0.365	6.405	-0.285	-0.650	6.720	0.030	-0.335	-0.0157
B	Bottom	6.535	6.535	0.000	6.140	-0.395	-0.395	6.180	0.040	-0.355	6.460	-0.280	-0.075	6.400	0.220	-0.135	-0.0063

### 3.2. Microclimatic parameter monitoring

Microclimate parameters (air temperature and humidity) in the El Bosque Gallery of Covadura Cave (Fig. 2A) were monitored by using dataloggers iButton of Maxim-ic (model DS1923-F5). This device comprises a temperature sensor and a hygrometer, both included in a stainless steel container, similar in size to a coin. The sensor is fixed to a plastic support hanging from a plastic thread, and uses a lithium battery with an average life time of up to 10 years, so electric connection is not needed. Resolution for temperature and humidity are  $\pm 0.06$  °C and  $\pm 0.04\%$ , respectively.

Sampling frequency was set at every hour. This ensures quick sensor equilibration with the cave air even when fast environmental changes occur. Temperature accuracy was also evaluated in the laboratory using a 1/100 mercury thermometer. The same operation was repeated in the cave several times for checking calibration and drift of the sensors.

Cave air monitoring was performed at 20 cm from the gallery floor from September 2012 to November 2013. Two sensors were running at the same site, as a data verification test. Additionally, a preliminary experiment in which simultaneous monitoring of microclimatic parameters of cave air close to the floor and near the ceiling was performed in January 2012, in order to investigate possible thermal stratification in this cave (Sanna et al., 2012a). Climatic parameters outside the cave were also measured using an iButton sensor for the period September 2012 to November 2013 (Figs. 6 and 7).

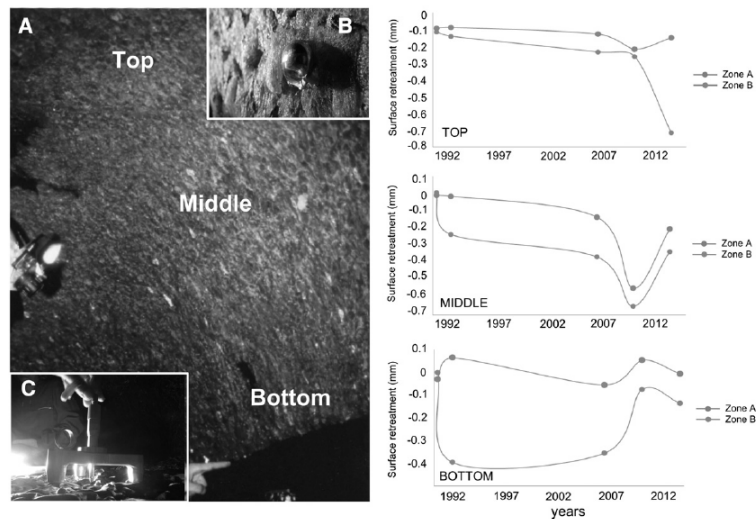


Fig. 4. A. Micro-erosion meter station at the “Laboratory Tunnel” of Cueva del Agua. B. Evidences of condensation on a MEM nail at the station on top; C. MEM device measuring gypsum surface retreatment. Two profiles composed of three MEM stations each (top, middle and bottom) were monitored over 21 years. MEM measurements of gypsum surface lowering are plotted for each station (photos by L. Sanna and Paolo Forti).

### 3.3. Direct measurement of condensation amount

Condensation water was collected in the wider part of El Bosque Gallery of Covadura Cave, 20 m from the entrance of this passage, by means of an assembly consisting of a metal plate (50 × 25 cm) placed at the height of 1.5 m from the cave floor (Fig. 5). This site was chosen because evidences of dissolution morphologies and active condensation on the cave ceiling had been previously detected (Sanna et al., 2012a).

In contrast, dripping points have not been observed in this area, but some hollow stalagmites are located 5 m into the gallery (Fig. 3D). The metal lamina was folded 90° along its long axis and placed with a 45° angle slope to favour the flow of condensation water (Fig. 5). The plate was supported by a wooden base and its inclined surface was placed perpendicular to the passage length and faced the gallery entrance. Theoretically, moist air coming from outside comes up against the metal plate and leaves water in the form of condensation.

Water dripping from the plate was collected using a plastic container coupled to a funnel 1 cm in diameter at its narrow part to minimise potential evaporation of the stored water. The sampling frequency ranged from 28 to 62 days, from July 2011 to November 2013. Water conductivity was measured in situ by a WTW handheld meter (Multi 340i: resolution 0.01 mS/cm, accuracy ±0.5%). Rainfall data in the Sorbas area were obtained from a nearby meteorological station (5 km away from Covadura Cave) part of the Automatic System of Hydrological Information (SAIH) of the Andalusia Government (Station #93, [www.redhidrosurmedioambiente.es](http://www.redhidrosurmedioambiente.es)).

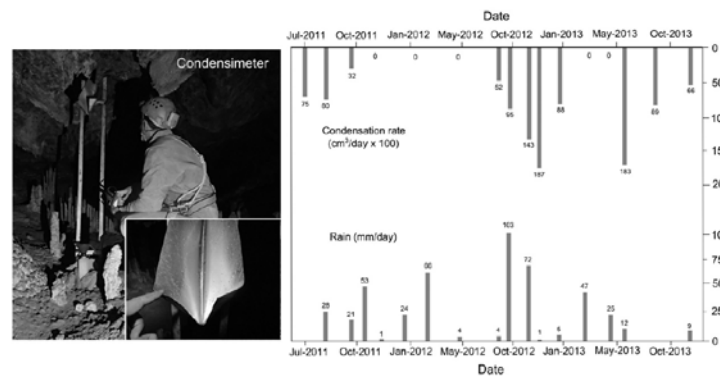


Fig. 5. Condensimeter in El Bosque Gallery of Covadura Cave. Condensation rates and rainfall in the Sorbas area between June 2011 and November 2013 (photos by J.M. Calaforra).

## 4. Results and discussion

### 4.1. Speleological evidence of condensation corrosion and related Mechanisms

Evidences of condensation processes are present in the upper cave galleries of the gypsum karst of Sorbas. In places, dissolution driven by condensation produces rounded shapes on the cave ceiling, in the form of semispherical cupolas, pendant-like features and smoothed surfaces on cave walls, which have been identified in Cueva del Agua and C3 Cave (Fig. 3A). Also very common is the presence of irregular ceiling forms composed of microcrystalline gypsum crystals as a result of heterogeneous and more aggressive dissolution of the gypsum host rock, as observed in some galleries of Cueva del Agua (Fig. 3B), at the entrance hall of C3 Cave and on the ceiling of El Bosque Gallery (Fig. 3D). In C3 Cave, dissolution forms appear in the upper parts of the passages, down to a level 1 m below the cave ceiling. Below this level the morphologies of the walls change drastically, and speleothems such as gypsum crusts, coraloids, and gypsum stalagmites are displayed. As for gypsum coraloids, popcorn-like speleothems appear on the cave walls showing a gradual decrease in size from around 1.5 m above the gallery floor, where only small new-formed gypsum crystals are observed, to gypsum botryoidal forms various centimetres in size and gypsum crusts that lie on the cave walls at the lower passage levels (Fig. 3F).

This size gradation represents differences in the supersaturation of the depositing water films, which can be put in relation with the speed at which evaporation occurs. These local differences are a result of the widespread mechanism of thermal stratification proposed in the current paper, which invokes warmer and wetter air in the upper parts of the cave passages and colder and drier air circulating in the lower parts. Hence, air entering the cave leaves condensation water in the upper parts, favouring gypsum dissolution and preventing secondary gypsum precipitation, whilst the evaporation and precipitation of gypsum speleothems take place along the lower parts of the cave walls (Fig. 3G). Gradations observed in the popcorn-like concretions in C3 Cave (Fig. 3F) and Covadura Cave indicate that the effects of thermal air stratification are reflected in gradual dissolution/evaporation processes in some locations.

Nevertheless, the transition between conditions for gypsum dissolution and those needed for gypsum precipitation appears to be abrupt in some sites of C3 Cave. In fact, 20-cm-thick crusts made of microcrystalline gypsum appear on the gypsum bedrock, whilst the upper part of the gypsum wall, above 1.5 m from the floor, is completely smoothed and apparently rounded by condensation corrosion. The boundary between the primary gypsum bedrock and the secondary gypsum crust is well defined. The upper part of the speleothem is rounded and re-dissolved by condensation mechanisms that gave rise to a concave-shaped surface (Fig. 3E). The genetic mechanism proposed here involves a first stage of gypsum host-rock dissolution by condensation in the upper part of the cave passage and migration of water saturated in calcium sulphate towards the lower wall parts, where the decreasing humidity produces evaporation and gypsum precipitation. In later stages, condensation became more intense at this cave site and the upper part of the gypsum crust was re-dissolved.

Similarly, gypsum “trees” with maximum heights of 50–60 cm appear in C3 Cave in a narrow passage 50 m far from the cave entrance. In contrast, the cave roof in this site is partially corroded and lacks speleothems (Fig. 3C). The presence of gypsum stalactites is limited to the entrance area (less than 20 m inside the cave) where evaporation is more intense and occurs even close to the cave ceiling. A similar pattern of dissolution and evaporation can be found in El Bosque Gallery. In this case, dissolution is evidenced by corroded gypsum surfaces and irregular pendant-like morphologies hanging from the cave ceiling (Fig. 3D). The presence of a group of carbonate stalactites covering the middle part of the gallery is particularly striking. These speleothems are currently active and their dripping generates one of the rarest gypsum speleothems of the Sorbas Caves, the hollow stalagmites (Fig. 3D) (Calaforra and Forti, 1993; Calaforra, 1996; Forti, 1996; Calaforra, 2003). Drops of condensation water can be found hanging on the cave ceiling, in particular in summer time. Like in C3 Cave, gypsum crusts and coralloids are abundant in this gallery below the height of 1 m from the floor, whereas the presence of gypsum stalactites and coralloids on the ceiling is limited to some sites close to the entrance area.

As in Cueva del Agua, smoothed surfaces at the top of the galleries have been identified, as well as rounded shapes related to dissolution produced by condensation water. Dissolved gypsum crystals from which water is dripping, as well as water drops on the MEM stations located in the “Laboratory Tunnel” (Fig. 4B), point to active condensation processes taking place in this cave.

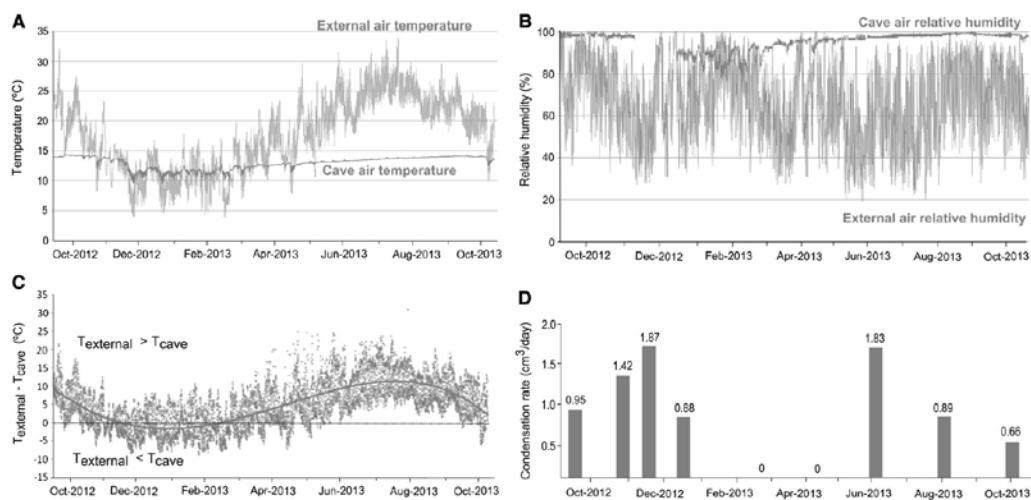


Fig. 6. A, B. Monitoring air temperature and humidity in El Bosque Gallery of Covadura Cave. External air temperature is also plotted (moving average, step = 15 data); C. difference between cave air temperature and external air temperature; D. condensation rate on a metal plate placed in El Bosque Gallery.

#### 4.2. Micro-erosion meter measurements

The overall gypsum surface retreat observed in the MEM station of the Laboratory Tunnel of Cueva del Agua ranged between  $-0.005$  and  $-0.705$  mm from 1992 to 2013 (Fig. 4 and Table 1), involving gypsum lowering rates ranging from  $-0.0002$  to  $-0.033$  mm yr $^{-1}$ . The highest dissolution rates correspond to MEM stations at the top and middle parts of the gypsum wall, in both Zones A and B, which range from  $-0.003$  to  $-0.033$  mm yr $^{-1}$ . In contrast, MEM stations located in the lower part of the wall underwent very slow gypsum dissolution rates, in particular in Zone A, where practically no gypsum erosion has been observed over the 21.4 years of this study ( $-0.0002$  mm yr $^{-1}$ ). These outcomes strongly support speleological observations mentioned above. Higher mean dissolution rates occur close to the passage ceilings, unlike sites closer to the cave bottom in which lowering of the gypsum surface is very subdued.

Taking into account all the MEM stations, the mean gypsum surface retreat was around  $-0.011$  mm yr $^{-1}$  during this long-term experiment. Calaforra (1996) reported gypsum dissolution rates of  $-0.1$  mm yr $^{-1}$  on average for these MEM stations in Cueva del Agua, during the period between 1992 and 1994. Calaforra's value is one order of magnitude higher than the one found during the complete experiment lasting 21.4 years. Such apparent discrepancy is a consequence of the relatively high gypsum surface lowering detected in the second reading (July 1994) at the middle and bottom stations of Zone B,  $-0.235$  and  $-0.395$  mm yr $^{-1}$ , respectively. This point reinforces the warning expressed by Ford and Williams (1989) regarding the interpretation and extrapolation of MEM results through time and space. Remarkably, the gypsum dissolution rates at bottom MEM stations displayed erratic behaviour during the entire monitoring period (Fig. 4).

Experiments based on weight loss of gypsum tablets in the same locations performed between 1991 and 1994 found that gypsum dissolution rates varied from 0 to  $-0.03$  mm yr $^{-1}$ , with a mean value of  $0.004$  mm yr $^{-1}$  (Calaforra, 1996; Klimchouk et al., 1996). These values are in total agreement with the ones obtained in our long-term MEM experiments. Similar gypsum dissolution rates based on gypsum tablet experiments were reported in Ukrainian gypsum caves ( $+0.03$  to  $-0.03$  mm yr $^{-1}$ ) (Klimchouk et al., 1996; Klimchouk and Aksem, 2002).

Between 1991 and 1994, MEM and gypsum tablet experiments were also carried out in locations of the Cueva del Agua affected by water flows, including perched cave lakes with occasional flooding, ephemeral cave streams and a sump at the downstream end of the cave system (Calaforra, 1996; Klimchouk et al., 1996). This early study found that the gypsum dissolution rate in these MEM stations ranged from  $-0.02$  to  $-0.16$  mm yr $^{-1}$  on average. This means that, in places, the gypsum surface lowering produced by condensation mechanisms may be greater than the one produced by sporadic or permanent streams flowing in gypsum caves. This is strongly supported by theoretical approaches that point to condensation as a very efficient mechanism of host rock dissolution in caves (Dublyansky and Dublyansky, 1998; Dreybrodt et al., 2005). This is due to low salinity of condensation water, which involves a great potential for gypsum dissolution. Hence, dissolution due to condensation is demonstrated to be an important process in gypsum cave evolution, especially in semi-arid zones (Klimchouk, 1996).

#### 4.3. Seasonal pattern of condensation

Monitoring of cave air temperature close to the floor of El Bosque Gallery in Covadura cave during the period 2012–2013 shows that higher air temperature values were recorded in late September, with maximum values of  $14.3$  °C and  $14.2$  °C in 2012 and 2013, respectively. On the other hand,

the lowest air temperatures, around 9.5 °C, were recorded in early December 2012 and the air remained cold at around 11.5 °C between December 2012 and March 2013. Then, air temperature started increasing gradually over spring and summer times. The mean air temperature during the whole period in this passage was 13.0 °C.

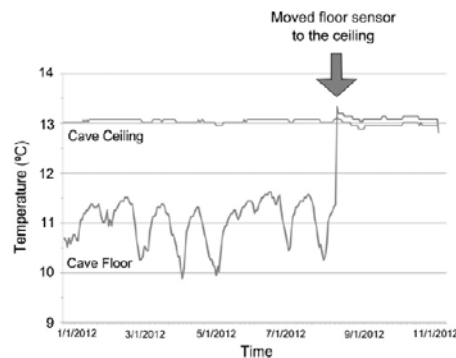


Fig. 7. Monitoring air temperature experiment performed during eleven days in El Bosque Gallery of Covadura Cave. Temperature was monitored close to the ceiling and at the bottom of the cave. On the eighth day, the floor sensor was moved besides the ceiling sensor.

The period of maximum air temperature values recorded outside occurred around July–August 2013, with maximum temperature of up 37.0 °C. Nevertheless, whilst external air temperature decreased from middle August, cave temperature in El Bosque Gallery continued rising until late September. This fact suggests that microclimate parameters are barely affected by external temperature during summer in these cave passages, acting as a “cold air trap”. The gradual cave air temperature increase during summer time could be a result of heating produced by condensation mechanisms, which is an exothermic process (585 kcal/kg), as well as, thermal diffusion from the surface.

On the other hand, the in-cave air temperature seems to be more strongly influenced by rapid cooling of the outside temperature than by extreme high-temperature events. For instance, relatively fast external air cooling in late October 2013 from 27 °C to 6 °C in only two days produced a cave temperature decrease of 1.4 °C, from 14.0 to 12.6 °C. This quick cave air cooling takes place as the outside atmosphere is colder than the in-cave air, so that cave air (relatively warmer with respect to the surface air masses) rises from the deepest parts of the cave and displaces air in its shallow passages. This process can have spectacular physical effects, as vapour columns coming out of the cave entrances during very cold days. In contrast, rapid outside temperature increases, as the one occurred in early October 2012 from 9 to 26 °C in three days did cause the underground air temperature to rise only 0.2 °C, suggesting that in periods in which the mean external air temperature is considerably higher than air temperature in El Bosque Gallery, air exchange in this passage is considerably limited, acting as a “cold air trap”. This is also supported by reduced temperature variability observed in the cave air during summer time in comparison with the high-frequency temperature oscillations occurring over winter time. This fact supports the above-mentioned mechanism of warming and heat accumulation in summer time because of water condensation on the cooler walls of the cave, which has also been observed in other cavities (Molerio and Leslie, 1981; Racovitca and Viemann, 1984).

The relative humidity record of the cave air is well correlated with the temperature. Relative humidity of cave air varied from 76 to 100%, with an average value of 95.6% during the entire period of monitoring. As for the air temperature, relative humidity of cave air reached its lower values in winter time, whilst it remained around 100% during summer. This suggests that colder air entering this passage during winter leads to drier conditions inside. It is worth mentioning that no correlation has been detected with respect to the relative humidity of external air. As noted by Klimchouk (1996), the intensity of air exchange and temperature differences between the outside and the in-cave atmosphere are most pronounced during warm seasons under temperate climatic conditions, and especially in semi-arid zones. On the other hand, colder and saturated air coming from deeper parts of the cave causes the upper cave level to become drier due to the reequilibration of its water vapour content at the warmer environment of the shallower passages. Deep air mass upward movement also triggers evaporation processes that locally removed heat.

In general terms, temperature gradients in ventilated conduits of caves are usually around 0.1 °Cm<sup>-1</sup> (Badino, 2010). Extreme temperature gradients of up to 5 °C m<sup>-1</sup> have been measured in grotta Cucchiara (Mt Kronio, Sicily), though this value represents a very special and very rare case in an active hydrothermal cave (Badino, 2010). This phenomenon is called thermal sedimentation and has also been observed in El Bosque Gallery in this work.

To this end, a temperature sensor that was initially placed close to the passage floor was moved to the upper part of the gallery, at a 2 m height, and at the same location of a second temperature sensor that was already measuring there. This experiment, carried out in the beginning of January 2012 (thus in winter conditions) demonstrated that air temperature close to the gallery roof was up to 3 °C higher than at the bottom (Fig. 7). Whilst air close to the upper cave conduit barely experienced daily temperature oscillations, differences of up to 1.5 °C were observed between day and night at the floor station. Thus the thermal gradient ranged between 0.75 and 1.5 °C m<sup>-1</sup> during the observation period. Most probably, this gradient undergoes variation during the year and is typical of this cave site. However, it is probable that this temperature gradient decreases during winter time due to increased air exchange and intake of colder air from outside and deeper parts of the cave during this season, as observed in other caves (Badino, 2010). Therefore, the temperature gradient due to thermal sedimentation in El Bosque Gallery during summer time is such that opposed mechanisms like condensation and evaporation can coexist in places only 2 m away.

Direct measurement of condensation in El Bosque Gallery found that the condensation rate presents systematic seasonal variations. Maximum condensation rate, up to 15 cm<sup>3</sup> m<sup>-2</sup> per day, takes place in summer and autumn (Figs. 5 and 6). The condensation rate starts decreasing during winter and no condensation was observed in late winter and early spring times. Non-condensation periods match in time with terms of reduced thermal differences between outside air and in cave air. In cases, external air was 10 °C colder than cave air (Fig. 5), so cave air masses from the deeper levels flowed towards upper passages, as well as colder air entered from lower entrances. As cold and relatively dry air arrives in the shallower conduits, there is an immediate transfer of sensible heat and vapour into the colder air because of the large heat and vapour gradient, and thus evaporation occurs (De Freitas et al., 1982).

The condensation experiment began in July 2011 and its record comprises over one year with data (January 2012–November 2013) which resulted in a condensation rate of 310 cm<sup>3</sup> yr<sup>-1</sup>. Taking into account the surface of the metal plate (0.125m<sup>2</sup>), this yields a specific condensation rate of 2480 cm<sup>3</sup>m<sup>-2</sup> yr<sup>-1</sup>, or 19.8mmyr<sup>-1</sup>. The lack of correlation between condensation rate and the annual distribution of rainfall amount in the Sorbas area (R<sub>2</sub>= 0.01) also supports the evidence of condensation phenomena (Fig. 6).

In situ conductivity analyses of collected condensation water ranged from 136 to 530 μS/cm, indicating relatively low concentration of dissolved salts in comparison with typical conductivity observed in waters of the gypsum karst of Sorbas, such as spring waters (2380 to 3290 μS/cm, Sanna et al., 2012b) and dripping water from stalactites in El Bosque Gallery (1670 to 3870 μS/cm). This corroborates that water collected in this experiment was almost exclusively produced by condensation and only a very small salt contribution from aerosols took place, as testified by foggy atmosphere observed in neutral periods. Condensation water with low concentration of dissolved salt presents a high potential to dissolve gypsum. In fact, a condensation rate of 2480 cm<sup>3</sup> m<sup>-2</sup> yr<sup>-1</sup> involves dissolution of 5.9 g m<sup>-2</sup> of gypsum per year (gypsum solubility at cave temperature being 2.40 g cm<sup>-3</sup>; Blount and Dickson, 1973). Estimation of gypsum dissolution rates caused by condensation in a particular zone of a gypsum cave in the Western Ukraine was found to vary from -0.001 to -0.005 mg cm<sup>-2</sup> per day according to the season (Klimchouk and Aksem, 2002), which implies that the

annual gypsum dissolution rates ranged between extreme values of 3.65 gm<sup>-2</sup> and 18.25 gm<sup>-2</sup>, in the range of data estimated for the gypsum karst of Sorbas.

In the Sorbas karst case, the gypsum dissolution rate produces the loss of 2.58 cm<sup>3</sup> m<sup>-2</sup> per year of gypsum (using a gypsum density of 2.31 g cm<sup>-3</sup>) that results in a gypsum surface lowering rate of 0.0026mmyr<sup>-1</sup>. This value is in the range of the lower gypsum dissolution rate observed by means of gypsum tablet experiments (0.004 mm yr<sup>-1</sup>, Calaforra, 1996; Klimchouk et al., 1996), and is also very similar to the surface lowering observed by MEM measurement at the highest (roof) stations of Zone A (0.0033 mm yr<sup>-1</sup>, Table 1).

## 5. Conclusions

Speleogen forms produced by condensation corrosion mechanisms have been identified in the gypsum karst of Sorbas. The upper cave passages show dissolutional forms on the ceilings, including corroded gypsum crystals, semi-spherical condensation domes and pendant-like morphologies.

Meanwhile, the lower part of the cave galleries are decorated frequently with spectacular gypsum crusts, stalagmites and coralloids, whose origin is linked to the evaporation of calcium-sulphate-rich waters. This suggests that condensation mechanisms are favoured close to the highest parts of the cave passages, whilst evaporation and gypsum precipitation is a widespread process near the cave floors. MEM measurements over a period of 21.4 years at different heights on a gypsum cave wall have corroborated these speleological evidences. The mean dissolution rate inferred by this method was 0.011mmyr<sup>-1</sup>. It was considerably higher closer to the passage ceiling than on the lower wall parts, where practically no gypsum surface lowering was observed.

Monitoring of microclimatic parameters (temperature and humidity) of cave air at the shallower cave levels indicates that warmer and moist air is located at the upper part of the cave passages, whereas the colder and drier air flows on the passage bottom. This thermal sedimentation is responsible for the condensation–evaporation mechanisms mentioned above.

Direct measurements of condensation waters support these microclimatic data. This periodic condensation–evaporation pattern suggests that the precipitation of gypsum speleothems in these caves depends on several factors (e.g. temperature, relative humidity, air circulation...) and evaporation areas are affected by seasonal cycles. As a general rule, secondary gypsum precipitation mainly occurs during winter, when cave air humidity is lower and evaporation is favoured. This behaviour presents relevant implications for future works using subaerial gypsum speleothems as palaeoclimatic proxies (Calaforra et al., 2008; Gázquez et al., 2011).

In addition, the condensation rates obtained on the basis of direct measurements on the metal plate (19.8 mm yr<sup>-1</sup>) have enabled us to estimate the mean gypsum dissolution rate occurred during the studied period (0.0026 mm yr<sup>-1</sup>), which is in the range of gypsum surface lowering observed by MEM measurements (0.0033 mm yr<sup>-1</sup>) and the one obtained by earlier experiments of gypsum tablet dissolution (0.004 mm yr<sup>-1</sup>). In cases, gypsum dissolution rates due to condensation are higher than the ones observed in passages partially flooded by permanent or temporary streams. Therefore, although one might think that water streams flowing in gypsum caves normally represent the main speleogenetical drivers, this investigation reveals that condensation must be taken into account as an important speleogenetic agent in gypsum caves in semi-arid areas, producing typical cave forms.

## Acknowledgements

Financial support of this work was made available through the Spanish Science grant AP-2007-02799 and the "GLOCHARID" Project of the Junta de Andalucía Regional Government (852/2009/M/00). The authors appreciate the photos provided by Jabier Les and thank the Speleoclub Almería (ECA) for its support during field work. Finally, the authors appreciate the suggestions made by Guest Editor Francisco Gutiérrez, Senior Editor Adrian Harvey and two anonymous reviewers, which helped to improve the original manuscript.

## References

- Audra, Ph., Bigot, J.Y., Mocochain, L., 2002. Hypogenic caves in Provence (France). Specific features and sediments. *Acta Carsol.* 31, 33–50.
- Audra, Ph., Hoblea, F., Bigot, J.Y., Nobécourt, J.C., 2007. The role of condensation in thermal speleogenesis: study of a hypogenic sulfidic cave in Aix-les-Bains, France. *Acta Carsol.* 36, 185–194.
- Audra, Ph., Mocochain, L., Bigot, J.Y., Nobécourt, J.C., 2009. The association between bubble trails and folia: a morphological and sedimentary indicator of hypogenic speleogenesis by degassing, example from Adaouste Cave (Provence, France). *Int. J. Speleol.* 38, 93–102.
- Auler, A.S., Smart, P.L., 2004. Rates of condensation corrosion in speleothems of semi-arid northeastern Brazil. *Speleogenesis Evol. Karst Aquifers* 2 (2) (2 pp.).
- Avramidis, P., Hong, J., Barnes, C., James, J.J., 2001. A new method of measuring condensation corrosion. *Proceeding of the 13th International Congress of Speleology, Brasilia (on cd)*.
- Badino, G., 2010. Underground meteorology: what's the weather underground? *Acta Carsol.* 39, 427–448.
- Bakalowicz, W.J., Ford, D.C., Miller, T.E., Palmer, A.N., Palmer, M.V., 1987. Thermal genesis of dissolution caves in the Black Hills, South Dakota. *Geol. Soc. Am. Bull.* 99, 729–738.
- Blount, C.W., Dickson, F.W., 1973. Gypsum–anhydrite equilibria in systems CaSO<sub>4</sub>–H<sub>2</sub>O and CaSO<sub>4</sub>–NaCl–H<sub>2</sub>O. *Am. Mineral.* 58, 323–331.
- Braga, J.C., Baena, J., Calaforra, J.M., Coves, J.V., Dabrio, C., Feixas, C., Fernández, J.M., Gómez, J.A., Goy, J.L., Harvey, A.M., Martín, J.M., Martín, A., Mather, A.E., Stokes, M., Villalobos, M., Zazo, C., 2003. In: Villalobos, M. (Ed.), *Geology of the Arid Zone of Almería, South-East Spain. An Educational Field Guide* (163 pp.).
- Calaforra, J.M., 1996. *Contribución al conocimiento de la karstología de yesos* (PhD Thesis) University of Granada, Spain (350 pp.).
- Calaforra, J.M., 2003. *El Karst en Yeso de Sorbas. Un recorrido subterráneo por el interior del yeso*. Ed. Publicaciones Calle Mayor S.L. (83 pp.).
- Calaforra, J.M., DeWaele, J., 2011. New peculiar cave ceiling forms from Carlsbad Caverns (New Mexico, USA): the zenithal ceiling tube-holes. *Geomorphology* 134, 43–48.
- Calaforra, J.M., Forti, P., 1993. Le palle di gesso e le stalagmiti cave: due nuove forme di concrezionamento gessoso scoperte nelle grotte di Sorbas (Andalusia, Spagna). *XVI Congresso Nazionale di Speleologia, Udine 1990*, vol. 1, pp. 73–88.
- Calaforra, J.M., Pulido-Bosch, A., 1996. Some examples of gypsum karst and the most important gypsum caves in Spain. *Int. J. Speleol.* 25, 225–237.
- Calaforra, J.M., Pulido-Bosch, A., 2003. Evolution of the gypsum karst of Sorbas (SE Spain). *Geomorphology* 50, 173–180.
- Calaforra, J.M., Dell'Aglio, A., Forti, P., 1993. Preliminary data on the chemical erosion in gypsum karst. The Sorbas region (Spain). *Proceedings of the 11th International Congress of Speleology (Beijing)*, pp. 97–99.
- Calaforra, J.M., Forti, P., Fernández-Cortés, A., 2008. Speleothems in gypsum caves and their palaeoclimatological significance. *Environ. Geol.* 53, 1099–1105.
- Cigna, A., Forti, P., 1986. The speleogenetic role of airflow caused by convection. 1<sup>st</sup> contribution. *Int. J. Speleol.* 15, 41–52.
- De Freitas, C.R., Schmekal, A.A., 2003. Condensation as a microclimate process: measurement, numerical simulation and prediction in the Glowworm tourist cave, New Zealand. *Int. J. Climatol.* 23, 557–575.
- De Freitas, C.R., Schmekal, A., 2006. Studies of corrosion/condensation process in the Glowworm Cave, New Zealand. *Int. J. Speleol.* 35, 75–81.
- De Freitas, C.R., Littlejohn, R.N., Clarkson, T.S., Kristament, I.S., 1982. Cave climate: assessment of airflow and ventilation. *Int. J. Climatol.* 2, 383–397.
- De Waele, J., Forti, P., 2006. A new hypogean karst form: the oxidation vent. *Z. Geomorphol.* 147, 107–127.
- De Waele, J., Mucedda, M., Montanaro, L., 2009. Morphology and origin of coastal karst landforms in Miocene and Quaternary carbonate rocks along the central-western coast of Sardinia (Italy). *Geomorphology* 106, 26–34.
- Dreybrodt, W., Gabrovšek, F., Perne, M., 2005. Condensation corrosion: a theoretical approach. *Acta Carsol.* 34, 317–348.
- Dronkert, H., 1976. Late Miocene evaporites in the Sorbas basin and adjoining areas. *Mem. Soc. Geol. Ital.* 16, 341–362.
- Dronkert, H., 1977. The evaporites of the Sorbas Basin. *Rev. Investig. Geol. Diput. Barcelona* 33, 55–76.
- Dublyanskaya, G.N., Dublyansky, V.N., 1989. The role of condensation in the development of mountain karst. *Problemi Kompleksnogo Izucheniya Karsta Gornikh Stran. Tbilisi- Tskhaltubo*, pp. 107–108 (In Russian).
- Dublyansky, V.N., Dublyansky, Y.V., 1998. The problem of condensation in karst studies. *J. Caves Karst Stud.* 60 (1), 3–17.
- Dublyansky, V.N., Dublyansky, Y.V., 2000. The role of condensation in karst hydrogeology and speleogenesis. In: Klimchouk, A.B., Ford, D.C., Palmer, A.N., Dreybrodt, W. (Eds.), *Speleogenesis, Evolution of Karst Aquifers*. National Speleological Society, Huntsville, pp. 100–111.

- Fernández-Cortés, A., 2005. *Caracterización microclimática de cavidades y análisis de la influencia antrópica de su uso turístico* (PhD Thesis) University of Almería, Almería (425 pp.).
- Fernández-Cortés, A., Calaforra, J.M., García-Guinea, J., 2006. The Pulpi gigantic geode (Almería, Spain): geology, metal pollution, microclimatology and conservation. *Environ. Geol.* 50, 707–716.
- Ford, D.C., Williams, P.W., 1989. *Karst Geomorphology and Hydrology*. Unwin Hyman, London (601 pp.).
- Forti, P., 1993. Karst evolution and water circulation in gypsum formations. In: Afrasiabian, A. (Ed.), *Proceedings of the International Symposium on Water Resources in Karst with Special Emphasis in Arid and Semi-arid Zones*, pp. 791–801 (Shiraz, Iran).
- Forti, P., 1996. Speleothems and cave minerals in gypsum caves. *Int. J. Speleol.* 25, 91–104.
- Gabrovšek, F., Dreybrodt, W., Perne, M., 2010. Physics of condensation corrosion in caves. In: Andreo, B., Carrasco, F., Durán, J.J., LaMoreaux, J.W. (Eds.), *Advances in Research in Karst Media*, Environmental Earth Sciences, pp. 491–496.
- Gázquez, F., 2012. *Registros paleoambientales a partir de espeleotemas yesíferos y carbonáticos* (PhD Thesis) University of Almería, Spain (381 pp.).
- Gázquez, F., Calaforra, J.M., 2013. Hypogenic speleogenesis and speleothems of Sima de la Higuera Cave (Murcia, South-eastern Spain). *Proceedings of the XVth International Congress of Speleology*, Brno, II, pp. 78–83.
- Gázquez, F., Calaforra, J.M., 2014. The gypsumkarst of Sorbas, Betic Chain. In: Gutierrez, F., Gutierrez, M. (Eds.), *Landscapes and Landforms of Spain*. Springer, Berlin, pp. 127–135.
- Gázquez, F., Calaforra, J.M., Sanna, L., Forti, P., 2011. Espeleotemas de yeso: ¿Un nuevo proxy paleoclimático? *Boletín de la Real Sociedad Española de Historia Natural. Sección Geol.* 105 (1–4), 15–24.
- Gázquez, F., Calaforra, J.M., Rull, F., 2012. Boxwork and ferromanganese coatings in hypogenic caves: an example from Sima de la Higuera Cave (Murcia, SE Spain). *Geomorphology* 177–178, 158–166.
- Gázquez, F., Calaforra, J.M., Forti, P., DeWaele, J., Sanna, L., Rull, F., Sanz, A., 2013. Corrosion of calcite crystals by metal-rich mud in caves: study case in Crovassa Ricchi in Argento Cave (SW Sardinia, Italy). *Geomorphology* 198, 138–146.
- Hill, C.A., 1987. Geology of Carlsbad Cavern and other caves in the Guadalupe Mountains, New Mexico and Texas: Socorro, NM. *Bull. New Mex. Bur. Min. Mineral Resour.* 117, 1–50.
- Jameson, R.A., 1991. Features of condensation corrosion in caves of the Greenbrier karst, West Virginia. *Natl. Speleol. Soc. Bull.* 53, 44.
- Klimchouk, A.B., 1996. Speleogenesis in gypsum. *Int. J. Speleol.* 25 (3–4), 61–82.
- Klimchouk, A.B., 2009. Morphogenesis of hypogenic caves. *Geomorphology* 106, 100–117.
- Klimchouk, A.B., Aksem, S.D., 2002. Gypsum karst in the western Ukraine: Hydrochemistry and solution rates. *Carbonate Evaporite.* 17, 142–153.
- Klimchouk, A.B., Cucchi, F., Calaforra, J.M., Aksem, S., Finocchiaro, F., Forti, P., 1996. Dissolution of gypsum from field observations. *Int. J. Speleol.* 25 (3–4), 37–48.
- Krijgsman, W., Fortuin, A.R., Hilgen, F.J., Sierro, F.J., 2001. Astrochronology for the Messinian Sorbas basin (SE Spain) and orbital (precessional) forcing for evaporite cyclicity. *Sediment. Geol.* 140, 43–60.
- LaRock, E.J., Cunningham, K.I., 1995. Helictite bush formation and aquifer cooling in Wind Cave, Wind Cave National Park, South Dakota. *Natl. Speleol. Soc. Bull.* 57, 43–51.
- Maestre, F.T., Escolar, C., Ladron de Guevara, M., Quero, J.L., Lazaro, R., Delgado-Baquerizo, M., Ochoa, V., Berdugo, M., Gozalo, B., Gallardo, A., 2013. Changes in biocrust cover drive carbon cycle responses to climate change in drylands. *Glob. Chang. Biol.* 19, 3835–3847.
- Mather, A.E., Martin, J.M., Harvey, A., Braga, J.C., 2001. *A field guide to the neogene sedimentary basin of the Almería Province, SE Spain*. Blackwell Science, Oxford, p. 229.
- Molerio, L., Leslie, F., 1981. *Hidrogeología y Climatología de la Cueva La Mariana*. Contribución al Estudio de las Cuevas de Calor. *Volunt. Hidrául.* XVIII (57), 2–9 (La Habana).
- Palmer, A.N., 2011. Distinction between epigenic and hypogenic caves. *Geomorphology* 134, 9–22.
- Pasini, G., 2012. Speleogenesis of the “Buco dei Vinchi” inactive swallow hole (Monte Croara karst sub-area, Bologna, Italy), an outstanding example of antigravitative erosion (or “paragenesis”) in selenitic gypsum. An outline of the “post-antigravitative erosion”. *Acta Carsol.* 41, 15–34.
- Pasquini, G., 1973. *Aggressive Condensation*. *Proceeding of the 6th International Congress of Speleology*, 8, pp. 315–318.
- Plan, L., Tschegg, C., DeWaele, J., Spötl, C., 2012. Corrosion morphology and cave wall alteration in an Alpine sulfuric acid cave (Kraushöhle, Austria). *Geomorphology* 169–170, 45–54.
- Racovitza, G., Viemann, J., 1984. *Sur le rôle de la condensation souterraine dans la genèse des stalagmites de glace*. *Trav. Inst. Spéol. E. Racovitza* 23, 89–97.
- Roep, Th.B., Beets, D.J., Dronkert, H., Pagnier, H., 1979. A prograding coastal sequence of wave-built structures of Messinian age, Sorbas, Almería, Spain. *Sediment. Geol.* 22, 135–163.
- Roveri, M., Gennari, R., Lugli, S., Manzi, V., 2009. The Terminal Carbonate Complex: the record of sea-level changes during Messinian salinity crisis. *GeoActa* 8, 63–70.
- Sanna, L., Calaforra, J.M., Gázquez, F., Pascucci, V., Andreucci, S., 2011. Sediments within Cueva C3 gypsum cave (Sorbas, SE Spain). *Geotitalia 2011 — VIII Italian Forum of Earth Sciences (Torino, Italy)*. *Epitome* 4, 253–254.
- Sanna, L., Gázquez, F., Calaforra, J.M., Fernández-Cortés, A., 2012a. Micrometeorology of Covadura Cave (SE Spain) as global change proxy. *20th International Karstological School (Postojna, Slovenia)*. *Guide Book & Abstracts*, pp. 74–75.
- Sanna, L., Gázquez, F., Calaforra, J.M., 2012b. A geomorphological approach in the study of hydrogeology of gypsum karst of Sorbas (SE Spain). *Geogr. Fis. Din. Quat.* 35, 153–166.
- Sarbu, S.M., Lascu, C., 1997. Condensation Corrosion in Movile Cave, Romania. *J. Caves Karst Stud.* 59, 99–102.
- Spate, A.P., Jennings, J.N., Smith, D.I., Greenaway, M.A., 1985. The micro-erosion meter— use and limitations. *Earth Surf. Process. Landf.* 10, 427–440.
- Stephenson, W.J., Finlayson, B.L., 2009. Measuring erosion with the micro-erosion meter — contributions to understanding landform evolution. *Earth Sci. Rev.* 95, 53–62.
- Stephenson, W.J., Kirk, R.M., Hemmingsen, S.A., Hemmingsen, M.A., 2010. Decadal scale micro erosion rates on shore platforms. *Geomorphology* 114, 22–29.
- Tarhule-Lips, R.F.A., Ford, D.C., 1998. Condensation corrosion in caves on Cayman Brac and Isla de Mona. *J. Caves Karst Stud.* 60, 84–95.
- Vattano, M., Audra, P., Benvenuto, F., Bigot, J.-Y., De Waele, J., Galli, E., Madonia, G., Nobécourt, J.-C., 2013. Hypogenic caves of Sicily (Southern Italy). In: Filippi, M., Bosak, P. (Eds.), *Proceedings of the 16th International Congress of Speleology*, Brno 19–27 July 2013, vol. 3, pp. 144–149.